Source mechanism of Astor Valley Earthquake of November 20, 2002 inferred from teleseismic body waves

TARIQ MAHMOOD, M. QAISAR & ZAHID ALI
Micro Seismic Studies Programme Ishfaq Ahmad Research Laboratories
P. O. Nilore, Islamabad

ABSTRACT: *Teleseismic body waves recorded at the IRIS Global Seismographic network are analyzed to investigate the source mechanism of the Astor valley earthquakes of Nov. 20, 2002 occurred in northern area of Pakistan about 60 km southeast of Gilgit near Bunji. The inversion method of Kikuchi and Kanamori is applied to the records of 11 seismic stations that included vertical P and horizontal SH components for this purpose. The azimuthal coverage of seismic stations was good enough to resolve some details of heterogeneous moment tensor. The fault area is estimated from the first four days aftershock distribution as 25 × 20 km² and their distribution corresponds to the local tectonic trends. The estimated seismic moment of the November 20, 2002 main shock is 9.4 × 10¹⁷ Nm which gives Mw = 5.9. The solution of body waves indicates normal faulting with a small component of strike slip on source fault whose strike is parallel to the local trend of MMT, with the tension axis perpendicular to it. The location of the main shocks along with aftershock area suggests that the nodal plane oriented southwest-northeast dipping to the northwest is preferred for the fault plane. Fault Plane solutions of November 01, 2002 and November 20, 2002 earthquakes derived from first motion polarity data recorded by MSSP local seismic network and some global seismic stations also show normal faulting. The results indicate that the Astor valley earthquakes may be considered to have occurred in an uncoupled region, in response to the gravitational pull due to internal gravity sliding.*

INTRODUCTION

On November 01, 2002 a moderate earthquake of magnitude $m_b = 5.3$ occurred in the northern area of Pakistan about 45 km southeast of Gilgit city. The earthquake occurred at 35°37' 12"N and 74°39' 36"E during local nighttime at 2209 GMT.

On November 20, 2002 the region was rocked again by another large shallow earthquake of magnitude $m_b = 6.2$ located on almost at the same location in the northwestern part of Astor valley, northern Pakistan during local nighttime. The main shock was followed by a large number of aftershocks, few of which were large enough to increase the damage caused by the main shock. The occurrence of aftershock lasted 40 days. This is the largest event ever recorded in the region. This earthquake provides a good opportunity to study the Seismotectonics characteristic of the region. The epicenter of main shock was located at about 60 km southeast of Gilgit city.

The epicenters of the earthquakes lie near the interface of Kohistan Magmatic Arc and the Nanga
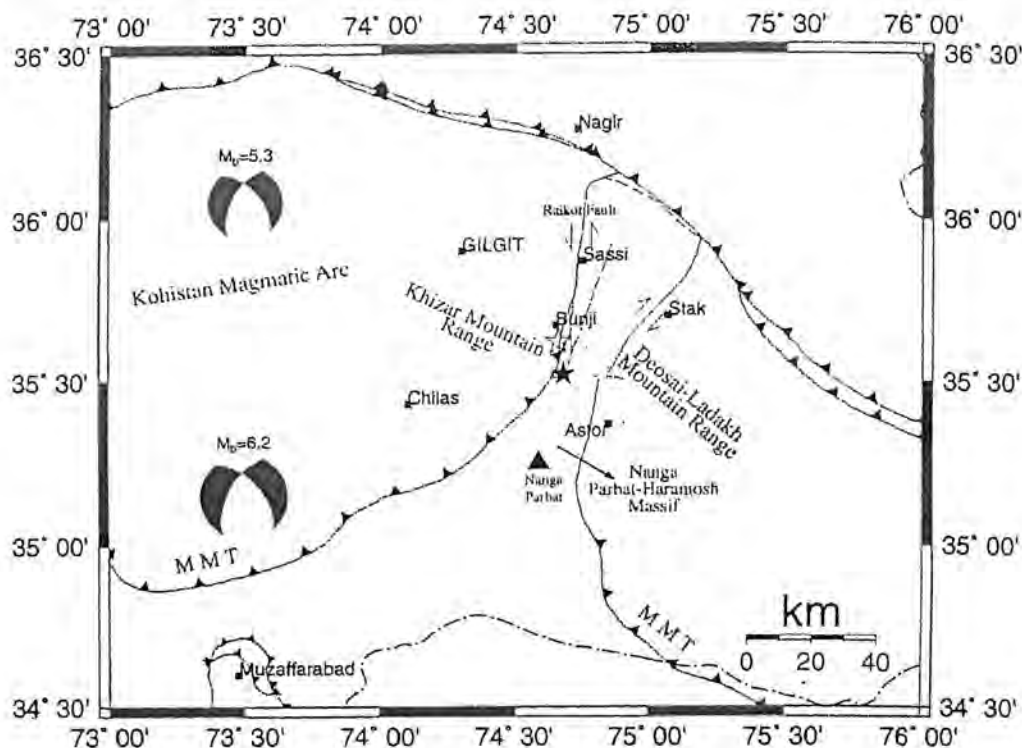
Fig. 1. Seismotectonic map of Gilgit and surrounding region modified from Geological Map of Pakistan by Farah
Hussain 1993 showing location of main shocks (stars) of November 20 and open star shows location of November
1, 2002.

Parbat Haramosh Massif, along the MMT-Raikot fault, near the town of Bunji (Fig. 1). The area also represents the northern margin of the under thrusting Indian plate. This feature raises the significance of the tectonic studies and study of active seismicity of the region. The entire area is faulted and fractured and seismically active with history of quite a few moderate-damaging earthquakes (Kazmi and Jan, 1997).

The main purpose of this study is to determine the mechanism of November 20, 2002 earthquake including, fault geometry, fault area, seismic moment and other related source parameters, using waveform inversion. Determination of these parameters is useful not only for understanding the physics of earthquakes but also for estimating the potential hazard associated with

stress changes in the faults adjacent to the earthquake area.

MAIN SHOCK AND AFTERSHOCKS

The hypocenter of the November 20, 2002 Astor valley earthquake was relocated by using computer code HYPOELLIPSE (Lahr, 1999). The data recorded by local seismic network and some global seismic stations for azimuthal coverage were used to determine the hypocentral parameters (Fig. 2). The following were the hypocentral parameter of the main shock.

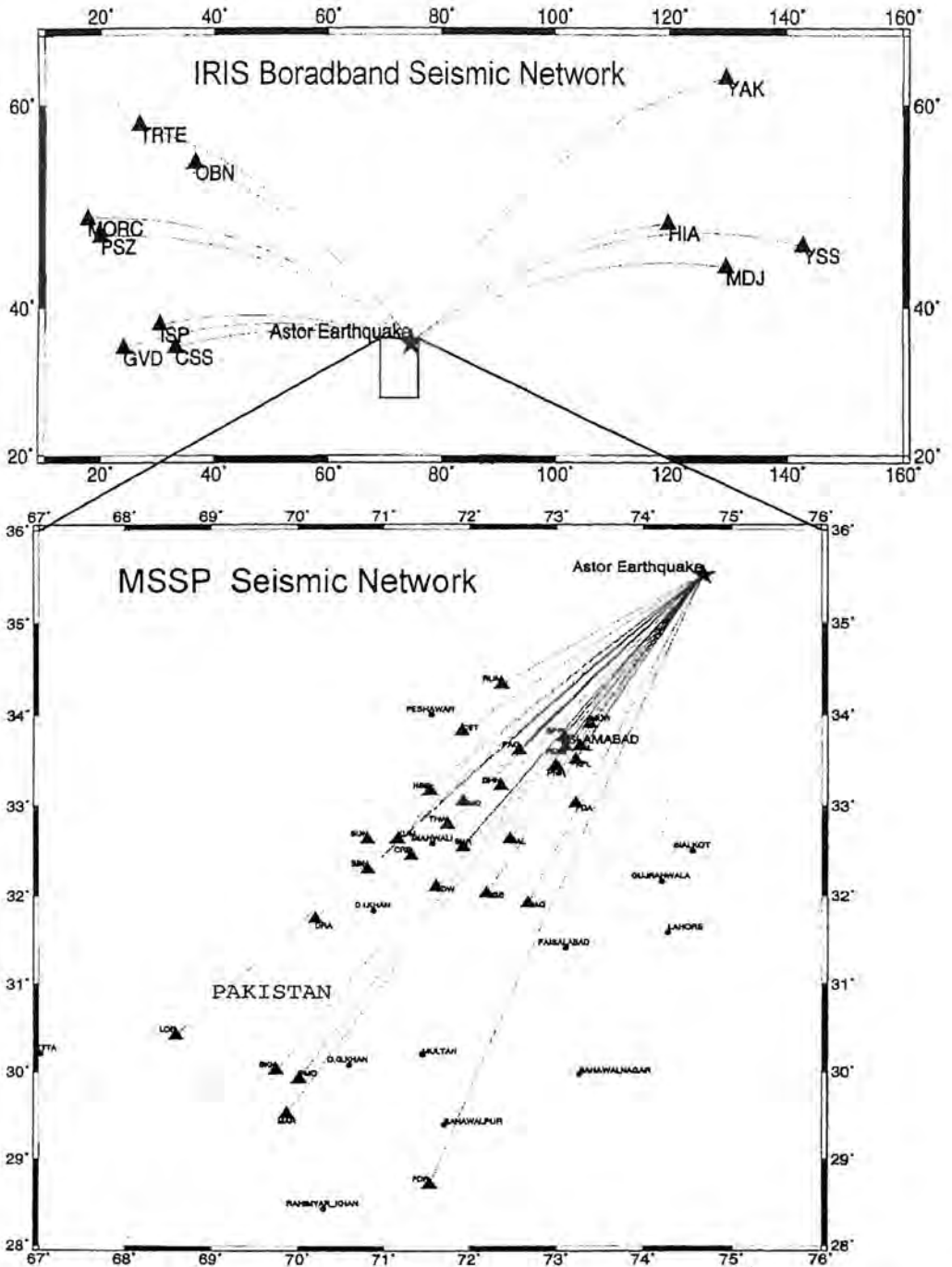|		
Origin time	:	21:32:29.85
Epicenter	:	35.52°N, 74.68°E
Depth	:	21.5 km
Magnitude (m_b)	:	6.2

Fig 2. MSSP seismic network and IRIS broadband seismograph stations used in the present waveform inversion. Star denotes the main shock of November 20, 2002 earthquake and the solid triangles denote the stations.

The location of the main shock along with aftershock is shown in (Fig. 3). The locations of aftershocks extend about 30 km along the MMT-Raikot fault zone and the depth down to about 20 km. The results were almost same as the National Earthquake Information Center (NEIC), USA locations. The aftershocks are distributed in northeast and southwest direction.

GEODYNAMICS OF REGION

Pakistan is characterized by extensive zones of high seismicity and contains several Seismotectonics features generated by an integrated network of active faults. The present earthquake occurred in northwestern extremity of Astor valley, close to the interface of Ghizar range and Ladakh mountain ranges as shown in Fig 1.

The study area lies within High Himalayas where the Nanga Parbat Haramosh Massif and Kohistan Magmatic Arc define the tectonic setup of the present earthquake region (Fig 1). It has been believed that the development of thrust and fold system in the region by continued compression since more than 55 million years, resulted in the formation of many complex antiform and synform structures linked by the micro to mega scale faults.

The main shock and distribution of aftershocks is mainly along the Raikot fault zone that separates the Nanga Parbat Haramosh Massif by Kohistan Magmatic Arc near the town of Bunji. This is an active seismic zone with frequent earthquakes of 3 to 5 magnitude with depth ranging from 50-100 km (Kazmi and Jan, 1997).
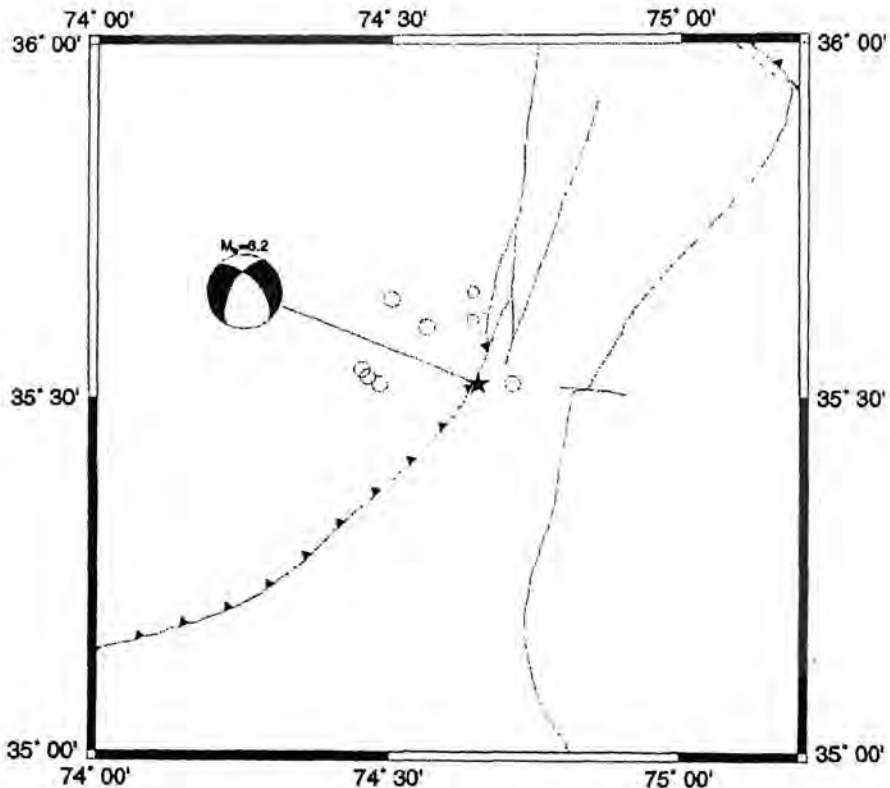

Fig. 3. Epicenter of main shock (star) of Nov 20, 2002 earthquake and it after shocks (circles) according to the size of the magnitude using MSSP data.
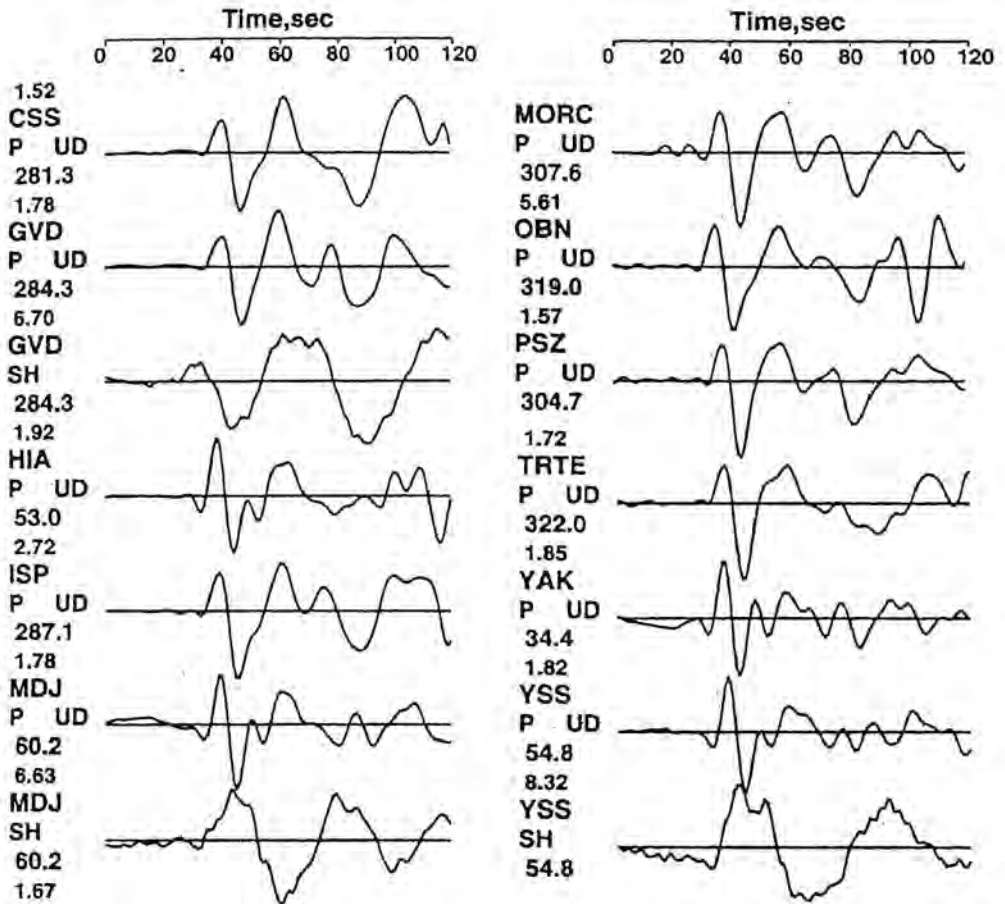
Fig. 4. Body waves recorded by IRIS stations used in the present waveform inversion for the Astor valley earthquake of Nov. 20, 2002.

Kohistan Magmatic Arc is an intraoceanic island arc bounded by the Indus Suture Zone or MMT to the south and the Shyoke Suture Zone or MKT to the north (Fig. 1). Gravity data modeling indicates that the MMT and MKT dip northward at 35° to 50° and that the Kohistan arc terrain is 8-10 km thick (Malinconics and Lillie, 1989). The seismological data suggests that arc is underlain by the Indian crustal plate (Seeber and Armbuster, 1979). The northern and western part of the arc, along MKT, is covered by a sequence of late Cretaceous to Paleocene volcanic and the arc terrain is mainly composed of igneous intrusions.

The Kohistan Magmatic Arc resulted when the Tethy Sea had begun to shrink by the time India began its northward drift around 130 million years ago. Intraoceanic subduction generated a series of volcanic arcs (Kohistan, Ladakh, Kandhar) during the Cretaceous era 136 to 65 m.y. (Searle, 1991). Continued subduction of the Tethy sea floor beneath Kohistan Ladakh arc and Eurasia, resulted in complete consumption of the leading oceanic edge of Indian plate and its eventual collision with remnants of the Kohistan-Ladakh arc. The abrupt slowing down of India's northward movement between 55 and 50 million years ago is attributed to this collision (Powell, 1979).
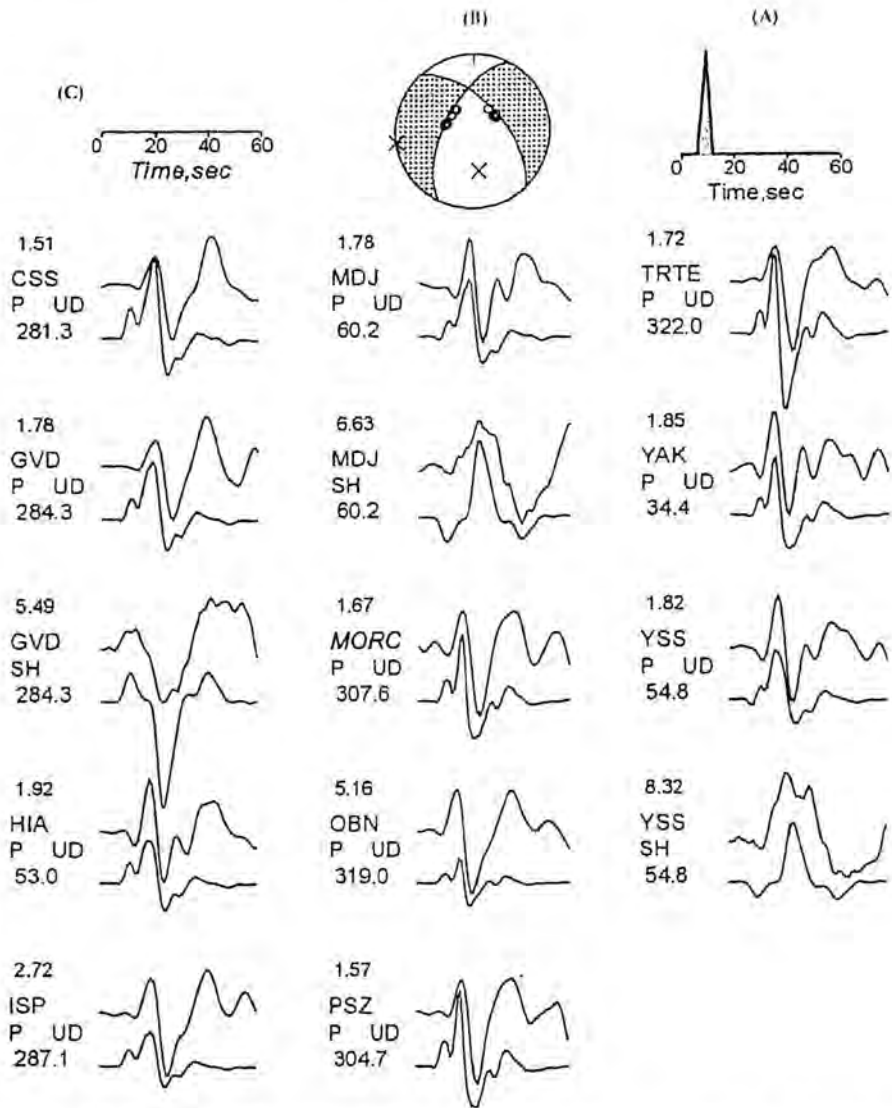
(C)

(B)

(A)

Fig. 5. Results of the inversion with double couple source. (A) Seismic moment release as a function of time (B) Mechanism of the best fit double couple point source (C) Observed and synthetic P and SH wave forms. The numbers in the upper and lower left indicate peak-to-peak amplitude in microns of the observed records and azimuth respectively.

The Nanga Parbat-Haramosh Massif is a major re-entrant into the Kohistan arc terrain. Treloar et al. (1991) have, however, shown that between Raikot and Sassi, the MMT is comprised of a complex system of thrusts and shears. According to various investigators (Tahirkheli 1979, Bard et al. 1980,

Coward et al. 1986, Butler et al. 1992), the MMT surrounds this massif. Madin (1986) and Madin et al. (1989) presented field evidence that along the western side of Nanga Parbat-Haramosh Massif there is an active dextral (right lateral strike slip) reverse fault-the Raikot Fault (Fig. 1) that truncates

MMT and forms the western boundary of the massif. Treloar et al. (1991) have, however, shown that between Raikot and Sassi, the MMT is comprised of a complex system of thrusts and shears.

The Nanga Parbat-Haramosh Massif is unique due to its current extraordinarily high uplift rate of over 5 mm/year (Kazmi and Jan, 1997). Fission-track and Ar^{40}/Ar^{39} data by Zeilter (1985) show that this uplift is 7 times higher than in the adjacent Kohistan arc terrain. Zeilter's data (1985) show that this massif has been uplifted approximately 16 km in the last 6 to 8 m.y. and that the uplift has accelerated exponentially. On the basis of reconstruction of the original stratigraphy and subsequent postulated erosion, Madin et al. (1989) estimate that the actual total uplift of Nanga Parbat may have been about 24 km.

BODY WAVE ANALYSIS

Seismic data

The teleseismic broadband data set used in this study was retrieved from Data Management Center of the Incorporated Research Institute of Seismology (IRIS-DMC) in the epicentral distance ranges between 30° and 90°. In this distance range, the waveforms are not contaminated by strong upper mantle or core phases (Kikuchi, 1995). Fourteen body wave records from 11 stations, including vertical P and horizontal SH components, were used in this study to derive the source process of this earthquake. Station parameters are given in Table 1 and displacement records of P waves as well as SH waves are shown in (Fig 4).

Using IASPEI (1991) Seismological travel time-tables, the teleseismic body waves data were windowed for one minute starting 10s before P-wave arrival or S-wave arrival. The information contained in this time window is adequate to resolve the source process. The data were deconvolved to ground displacement and filtered with an appropriate fre-

quency band. The bandwidth is determined by considering the spectral content and noise level. A bandwidth of 0.02 to 5 Hz is used. The azimuthal coverage is good enough to resolve some details of the moment distribution.

Teleseismic body wave inversion

An iterative deconvolution inversion method developed by Kikuchi and Kanamori (1991) for teleseismic data is employed to resolve the source complexity by minimizing the difference between the observed and synthetic waveforms. In the first instance the source mechanism is determined with the approximations of a single point source such that synthetic waveforms are best fit with the observed ones. A three layer structures (two layers of crust and a semi-infinite mantle) is used for the synthetic waveform following the crustal model determined by (Qaisar et. al 1991) with only a minor modification in the source region as given in Table 2. The Green's function is calculated for the six element of the moment tensor at different depths beneath the epicenter with the assumption of a single point source. The focal depth lies within 20-25 km depth range. In order to get a more realistic waveform, the effects of inhomogenity in the structure, attenuation during traveling of waves and instruments response was considered. For attenuation parameter Q a Futterman (1962) operator t* (ratio of travel time to average Q) of 1s was used for P waves and 4s for S waves (Helmberger, 1983). This Q parameter was convolved with a triangular source time function having rise time τ_1 of 3s, source duration τ_2 of 6s and the seismic moment of ×10^{18} Nm. Consequently the seismograms were simultaneously inverted to double couple single point source in the least square sense for the source model parameter, assuming no change in the mechanism during rupture. The inversion process was carried over different depths. The depth yielding the minimum residual was taken as the depth of the source.

For this event a point source model provides more or less equal fits to most of the waveforms. This

TABLE 1

LIST OF STATION PARAMETERS

Station Name	Code	Azimuth	Back Azimuth	Delta	P	1/r	Phase	Weight
Mathiatis Cyprus	CSS	281.3	76.8	33.4	0.079	9.80	P-UD	1.0
Gardos Greece	GVD	284.3	73.9	40.8	0.074	9.74	P-UD	1.0
Gardos Greece	GVD	284.3	73.9	40.8	0.128	9.74	SH	0.2
Hailar China	HIA	53.0	-95.5	35.5	0.077	9.30	P-UD	1.0
Isparta Turkey	ISP	287.1	80.0	35.0	0.077	9.70	P-UD	1.0
Mudanjiang China	MDJ	60.2	-82.6	42.3	0.073	8.50	P-UD	1.0
Mudanjiang China	MDJ	60.2	-82.6	42.3	0.126	8.50	SH	0.2
Morovsky Czech. Republic	MORC	307.6	86.9	43.1	0.073	8.50	P-UD	1.0
Obninsk Russia	OBN	319.0	111.2	32.5	0.079	9.70	P-UD	1.0
Piszkes Hungary	PSZ	304.7	86.6	41.7	0.073	9.50	P-UD	1.0
Tortu Estonia	TRTE	322.0	105.3	38.7	0.075	9.50	P-UD	1.0
Yakutsk Russia	YAK	34.4	-101.7	43.0	0.073	8.40	P-UD	1.0
Yuzhno Russia	YSS	54.8	-76.9	50.9	0.068	7.80	P-UD	1.0
Yuzhno Russia	YSS	54.85	-76.9	50.9	0.118	7.80	SH	0.2

Where

Back Azimuth = Azimuth from station to source P = Ray Parameter (P = Sin i/v where i = angle of incidence)

1/r = Geometrical factor (×1/10 km),   Delta = Distance in degrees

TABLE 2

NEAR SOURCE STRUCTURE USED IN THE
WAVEFORM INVERSION

V_P	V_s	ρ	D
5.57	3.36	2.65	15
6.50	3.74	2.87	33
8.10	4.68	3.30	–

Where V_P, V_s = P-wave and S-wave velocities (km/s)
ρ = density (10^3 kg/m³);   D = thickness (km)

means that a single point source is sufficient to describe the source process of this earthquake. The P wave records as well as the SH waves, at different stations (Fig. 4) also reflect a smooth rupture. The fit of data i.e. synthetic and observed waveforms for the point source model is shown in (Fig. 5a-c). The final residual waveform error is 0.6224. The best matching double couple has a strike of 207.6°, a dip of 60.3° in the northwest direction and a slip of -36.2°, normal faulting mechanism.

Moreover, inversion was done using this solution as a fixed mechanism with the result indicating a good fit to the data with a final residual error equal to 0.6224. A slight change in the parameters of the fault plane caused an increase in the residual error. The final parameters of this solution are summarized in Table 3.

Stress drop

The local stress drop $\Delta\sigma_1$ is derived for the main shock from the seismic moment M_0 and rupture duration 2τ. In the present model a triangular source time function and half the duration τ that corresponds to the rise time of 3 sec is assumed. The local stress drop is estimated by using the relation of Fukao and Kikuchi (1987).

$$\Delta\sigma_1 = 2.5\, M_0/(V\tau)^3$$

Where V is the rupture velocity and τ represents the rupture duration. The rupture velocity is taken as V = 3.0 km/sec. The local stress drop is evaluated as $\Delta\sigma_1$=3Mpa for τ = 3 sec and $M_0 = 9.4 \times 10^{17}$ Nm. The aftershock area was estimated roughly as 25 × 20 km² by considering the aftershock occurred within 4 days. The average stress drop $\Delta\sigma$ was obtained by applying the relation (Fukao and Kikuchi, 1987).

$$\Delta\sigma = 2.5\, M_0 / S^{3/2}$$

The average stress drop is estimated as 0.2 Mpa for an aftershock area. It is observed that the local stress drop is higher than the average stress drop over the fault plane of 25 × 20 km². According to the slip dislocation theory of faulting (Aki, 1966) the average dislocation ($\bar{D}$) can be estimated by using the following relation

$$D = M_0 /\mu S$$

Where μ is the rigidity (3×10^{10} N/m²). The displacement 'D' is estimated as 0.063 m.

TABLE 3

FINAL SOURCE PARAMETERS

	Φ	δ	λ	H	M_o	M_w	σ_1	τ_1	τ_2
				(km)	(Nm)		(Mpa)	(sec)	(sec)
This Study	207.6	60.3	-36.2	21.5	9.4×10^{17}	5.9	3.2	3	6
Harvard CMT	202.0	26.0	-120	17.5	3.8×10^{17}	6.3			
USGS	230.0	43.0	-54	21.0	9.3×10^{17}	6.0			

Where Φ = Strike; δ = Dip; λ = Slip;   H = Depth M_o = Seismic moment; M_w = Moment magnitude;
σ_1 = Local Stress drop; τ_1 = Rise time; τ_2 = Source duration

DISCUSSIONS AND CONCLUSIONS

The earthquake of Nov. 20, 2002 was located in northwestern extremity of Astor valley, near the town of Bunji. Waveform analysis and aftershocks distribution reveal that the event represents normal faulting with a small component of strike-slip on source fault with strike $= 207.6°$, dip $= 60.3°$ northwest direction and slip $= -36.2°$. The seismic moment is 9.4×10^{17} Nm that correspond to a moment magnitude of 5.9.

The focal mechanism solution of Nov 20,2002 earthquake as determined by inversion method indicates normal faulting. Fault Plane solutions of Nov. 01, 2002 and Nov. 20, 2002 earthquakes derived from first motion polarity data recorded by MSSP local seismic network and some global seismic stations also show normal faulting. The strike of both the source faults is nearly close to the trace of Raikot fault but nature of fault i.e. normal, and is not appropriate to the general trend of the local tectonics that is dominated by collisional tectonics mostly strike-slip and thrust faulting.

The possible reason of normal faulting in Nanga Parbat-Haramosh Massif is that when the limbs of antiform reach at high-dip-angle, they are likely to become unstable under the gravity pull. This may ultimately initiate normal faulting by internal "gravity sliding". As describe earlier that the Nanga Parbat-Haramosh Massif has been uplifted about 16 km during the last 6 to 8 m.y. This uplift provides sufficient base for the activation of internal gravity sliding. The movement along Raikot fault zone where the strike slip component is dominant can provide threshold energy to activate the gravity sliding of high-dip-angle limb of an antiform/up-lifted structure of the region. This ultimately formed the source of the Astor valley seismic activity.

REFERENCES

Aki, K., 1966. Generation and propagation of G waves from the Niigata earthquake at June 16, 1964. Bull. Earthquake Res. Inst., Tokyo Univ., 44, 73-88.

Bard, J. P., Maluski, H., Matte, P. & Proust, F. 1980. The Kohistan sequence; Crust and mantle of an abducted island arc. Geol. Bull. Univ. Peshawar, 13, 87-93.

Butler, R. W. H., George, M., Harris, N. B. W., Jones, C., Prior, D. J., Treloar, P. J. & Wheeler, J., 1992. Geology of the northern part of Nanga Parbat massif, northern Pakistan, and its implications for Himalayan tectonics. J. Geol. Soc. Lond., 149, 557-567.

Coward, M. P., Windley, B. F., Broughton, R. D., Luff, I. W., Petterson, M. G., Pudsey, C. J., Rex, D. C. & Khan, M. A., 1986. Collision tectonics in the NW Himalayas. In: Coward, M. P., & Ries, A. C. (eds) Collision Tectonics. Geol. Soc. Lond., Spec. Publ., 19, 203-219.

Fukao, Y. & Kikuchi, M., 1987. Source retrieval for mantle earthquakes by iterative deconvolution of long period P-waves. Tectonophysics, 144, 249-269.

Futterman, W.I., 1962. Dispersive body wave. Journal of Geophysics. Res., 67, 5279-5291.

Helmberger, D.V., 1983. Theory and application of synthetic seismograms, in Earthquakes, Observation, Theory and Interpretation (Societa Italiana di Fisica, Bologna, Italy), 174-222.

Hussain, F., 1993. Geological Map of Pakistan. Pub: Geological Survey of Pakistan, Quetta, Pakistan.

Kazmi, A. H. & Jan, M. Q., 1997. Geology and Tectonics of Pakistan. Graphic Publishers, Nazimabad, Karachi, 160, 410-413.

Kennett, B. L. N., 1991. IASPEI 1991 Seismological Tables. Research School of Earth Sciences, Australian National University, Canberra ACT 2601, Australia.

Kikuchi, M. & Kanamori, H., 1991. Inversion of complex body waves –III. Bull. Seismol. Soc. Am., 79, 670-689.

Kikuchi, M., 1995. "Notes on Earthquake Source Process" IISEE, JICA, Japan, 1-97.

Lahr, J.C., HYPOELLIPSE: 1999. "A computer Programme for Determining Local Earthquake Hypocentral Parameters, Magnitude and First Motion Pattern." USGS Open File Report, 99-23.

Madin, I. P., 1986. Geology and neotectonics of the north-western Nanga Parbat-Haramosh Massif. M. S. thesis, Oregon State Univ., Corvallis, 160.

Madin, I. P., Lawrence, R. D., & Rehman, S., 1989. The north-western Nanga Parbat-Haramosh Massif; evidence for crustal uplift at the northwestern corner of the Indian Craton. In: Malinconics, L. L. & Lillee, R. J. (eds.) Tectonics of the Western Himalayas. Geol. Soc. Am., Spec. Pap., 232, 169-182.

Powell, C. M., 1979. A Speculative Tectonic History of Pakistan and Surroundings: some constrains from the Indian Ocean. In Geodynamics of Pakistan.. Farah, A. & DeJong, K. A. (Eds.) Geological Survey of Pakistan, Quetta, 5-24.

Qaisar, M., Shahid, M. B., Tariq, M. & Mubarak, M. A., 1991. Simultaneous inversion of velocity structure and hypocentral locations: Application to the area around the proposed Kalabagh Dam site, Pakistan. MSSP-41/91.

Searle, M. P., 1991. Geology and tectonics of the Karakoram Mountains. J. Wiley & Sons, New York, 358.

Seeber, L. & Armbruster, J., 1979. Seismicity of the Hazara arc in northern Pakistan: decollement versus basement faulting. In: Farah, A. & DeJong. K. A. (eds.) Geodynamics of Pakistan. Geol. Surv. Pak. Quetta, 131-142.

Tahirkheli, R. A. K. 1979. Geology of Kohistan and Adjoining Eurasian and Indo-Pakistan Continents. Geol. Bull. Univ. Peshawar, Pakistan, 20, 209-214.

Treloar, P. J. & Coward, M. P., 1991. Indian plate motion and shape: constrains on the geometry of the Himalayan Orogen. Tectonophysics, 191, 189-190.

Troxel, B. W. & Wright, L.A. 1987. Tertiary Extensional Features, Death Valley Region, Eastern California. Geol. Soc. Am. Centennial Field Guide-Cordilleran section.

Zeilter, P. K., 1985. Cooling history of the NW Himalaya, Pakistan. Tectonics, 4, 127-151.